typeset using JPSJ.sty <ver.0.7f>

Magnetic Phase Transition of the Perovskite-type Ti Oxides

Masahito MOCHIZUKI and Masatoshi IMADA

Institute for Solid State Physics, University of Tokyo,
5-1-5 Kashiwa-no-ha, Kashiwa, Chiba 277-8581

(Received February 1, 2008)

Properties and mechanism of the magnetic phase transition of the perovskite-type Ti oxides, which is driven by the Ti-O-Ti bond angle distortion, are studied theoretically by using the effective spin and pseudo-spin Hamiltonian with strong Coulomb repulsion. It is shown that the A-type antiferromagnetic(AFM(A)) to ferromagnetic(FM) phase transition occurs as the Ti-O-Ti bond angle is decreased. Through this phase transition, the orbital state is hardly changed so that the spin-exchange coupling along the c-axis changes nearly continuously from positive to negative and takes approximately zero at the phase boundary. The resultant strong two-dimensionality in the spin coupling causes a rapid suppression of the critical temperature as is observed experimentally.

KEYWORDS: perovskite-type Ti oxides, $GdFeO_3$-type distortion, d-level degeneracy, orbital ordering, second-order perturbation theory, A-type antiferromagnetism, Mermin and Wagner's theorem

§1. Introduction

Perovskite-type Ti oxide $R\mathrm{TiO_3}$(R being a trivalent rare-earth ion) is a typical Mott-Hubbard insulator[1]. $\mathrm{Ti^{3+}}$ has a $3d^1$ configuration, and one of the three-fold t_{2g} orbitals is occupied at each transition-metal site. The crystal structure is an orthorhombically distorted perovskite ($GdFeO_3$-type distortion) whose unit cell contains four octahedra as shown in Fig. 1. The magnitude of the distortion depends on the ionic radii of the R ion. With a small ionic radius of R ion, the lattice structure is more distorted and the bond angle is decreased more largely from 180°. The bond angle can be controlled by use of the solid-solution systems $\mathrm{La_{1-y}Y_yTiO_3}$ or in $R\mathrm{TiO_3}$, varying the R ions. Especially, with varying the Y concentration in $\mathrm{La_{1-y}Y_yTiO_3}$, we can control the bond angle almost continuously from 156° ($y = 0$) to 140° ($y = 1$). In $\mathrm{YTiO_3}$, a d-type JT distortion has been observed where

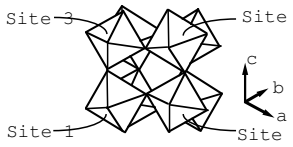

Fig. 1. $GdFeO_3$-type distortion.

the longer and shorter Ti-O bond lengths are $\sim 2.08\mathring{A}$ and $\sim 2.02\mathring{A}$, respectively[2]. Although the difference between the longer and shorter bond length is relatively small, $LaTiO_3$ also shows a d-type JT distortion. Recently, electronic and magnetic phase diagrams have been investigated intensively as functions of the magnitude of a Ti-O-Ti bond angle distortion [3,4,5,6]. In the less distorted or a La-rich($y < 0.6$) region, the system shows AFM ground state. In particular, $LaTiO_3$ ($y = 0.0$) shows a G-type AFM(AFM(G)) ground state with a magnetic moment $0.45\mu_B$[7]. With increasing the Y-concentration or varying the R site with smaller size ion (decrease of the Ti-O-Ti bond angle), the Nèel temperature (T_N) decreases rapidly and is suppressed to almost zero, and subsequently a FM ordering appears. This rapid decrease of T_N is hardly explained by the conventional models. The origin is one of the issues of interest. In the relatively distorted or Y-rich region, the system shows a FM ground state. In $YTiO_3$($y = 1.0$), the value of the magnetic moment is $0.84\mu_B$[8]. This ferromagnetism is hardly explained by a simple single-band Hubbard model and requires to consider the d-level degeneracy. Recent model Hartree-Fock studies have succeeded in reproducing the magnetic structures of the both end compounds[9,10]. The nature of the magnetic phase transition is, however, not sufficiently clarified. Besides, the spin and orbital states realized in the moderately distorted region are issues of interest. In this paper, we study the properties and mechanism of the phase transition by focusing on the region near the phase boundary.

§2. Formalism

We start with the multi-band d-p model in which the full degeneracies of Ti $3d$ and O $2p$ orbitals as well as on-site Coulomb and exchange interactions are taken into account. In this Hamiltonian, the effects of the $GdFeO_3$-type distortion are considered through the d-p transfer integrals which is defined by using the Slater-Koster's parameters $V_{pd\pi}$,$V_{pd\sigma}$,$V_{pp\pi}$ and $V_{pp\sigma}$[11]. The effects of the d-type Jahn-Teller(JT) distortion are also considered. The magnitude of the distortion is expressed by the ratio $[V^s_{pd\sigma}/V^l_{pd\sigma}]^{1/3}$, here $V^s_{pd\sigma}$ and $V^l_{pd\sigma}$ are the transfer integrals for the shorter and longer Ti-O bonds. In order to reveal the origin of the rapid suppression of T_N, we focus on the situation near the phase boundary between AFM

and FM phases. The value of the ratio $[V^s_{pd\sigma}/V^l_{pd\sigma}]^{1/3}$ is fixed at 1.030, which is expected to be realized near the phase boundary under the assumption of the linear increase as a function of the bond angle from 1.036($YTiO_3$) to 1.00($LaTiO_3$). Under the JT distortion, the t_{2g} level-splitting energy $\Delta_{t_{2g}}$ is estimated as 0.050eV by using Slater-Koster's relations. Since the t_{2g} level-splitting due to the spin-orbit interaction is sufficiently small in comparison with $\Delta_{t_{2g}}$, we neglect the interaction through the present calculations. By integrating over the O $2p$ orbital degrees of freedom, we derive the $effective$ Hubbard model which includes only Ti $3d$ orbital degrees of freedom.

Under the cubic-type crystal field, a five-fold degeneracy of $3d$ orbitals is lifted to two-fold higher levels e_g and three-fold lower levels t_{2g}. Moreover, in the d-type JT distortion, the degeneracies of the e_g and t_{2g} orbitals are lifted. Although the e_g level is uniformly lifted to a higher level $3z^2-r^2$ and a lower level x^2-y^2 at each site, the ways of t_{2g}-level splitting are different between sites 1, 3 and sites 2, 4 (see Fig. 1). In sites 1 and 3, the y-axis is elongated and consequently, the t_{2g} level is lifted to lower xy and yz levels and a higher zx level. On the other hand, in sites 2 and 4, the x-axis is elongated so that it is lifted to lower xy and zx levels and a higher yz level. Let us represent the five $3d$ orbitals xy, yz, zx, x^2-y^2 and $3z^2-r^2$ by energy-level indices 1, 3, 2, 4 and 5, respectively at sites 1 and 3, and by indices 1, 2, 3, 4 and 5 at sites 2 and 4. As a result, in the insulating d^1 systems under a JT distortion, one of the two-fold degenerate lower t_{2g} orbitals is occupied at each site. Especially, in the case of the d-type JT distortion, either xy or yz orbital is occupied at site 1 and 3, xy or zx at site 2 and 4.

Based on the above discussion, the multi-band Hubbard Hamiltonian derived from the multi-band d-p model has a form,

$$H^{\rm mH} = H_d^{\rm mH} + H_{tdd}^{\rm mH} + H_{\rm on-site} \tag{1}$$

with

$$H_d^{\rm mH} = \sum_{i,m,\sigma} \varepsilon_{d\,i,m} d^\dagger_{i,m,\sigma} d_{i,m,\sigma}, \tag{2}$$

$$H_{tdd}^{\rm mH} = \sum_{i,m,i',m',\sigma} t^{dd}_{im,i'm'} d^\dagger_{i,m,\sigma} d_{i',m',\sigma} + {\rm h.c.}, \tag{3}$$

$$H_{\rm on-site} = H_u + H_{u'} + H_j + H_{j'}, \tag{4}$$

where $d^\dagger_{i,m,\sigma}$ is a creation operator of an electron with spin $\sigma(=\uparrow,\downarrow)$ in a $3d$ level m at Ti site i. By $H_d^{\rm mH}$, we express the level energies of Ti $3d$ orbitals under the influence of the

crystal fields with

$$\varepsilon_{d\,i,m} = \begin{cases} \varepsilon_{dl} & \text{for} \quad m = 1, 3, \\ \varepsilon_{dl} + \Delta_{t_{2g}} & \text{for} \quad m = 2, \\ \varepsilon_{dl} + \Delta_{x^2-y^2} & \text{for} \quad m = 4, \\ \varepsilon_{dl} + \Delta_{3z^2-r^2} & \text{for} \quad m = 5. \end{cases} \tag{5}$$

Here, $m = 1, 3$ are lower t_{2g} levels, $m = 2$ is a higher t_{2g} level and $m = 4$ and $m = 5$ are lower and higher e_g levels, respectively. The $\Delta_{t_{2g}}$, $\Delta_{x^2-y^2}$ and $\Delta_{3z^2-r^2}$ denote the level-splitting energies measured from lower t_{2g} level. It should be noted that the same indices of energy levels at different sites do not necessarily correspond to the orbitals with the same symmetry. $H_{tdd}^{\rm mH}$ is a d-d super-transfer term and $H_{\rm on-site}$ represents on-site d-d Coulomb interactions. The $H_{\rm on-site}$ term consists of the following four contributions,

$$H_u = \sum_{i,m} u d^\dagger_{i,m,\uparrow} d_{i,m,\uparrow} d^\dagger_{i,m,\downarrow} d_{i,m,\downarrow}, \tag{6}$$

$$H_{u'} = \sum_{i,m>m',\sigma,\sigma'} u' d^\dagger_{i,m,\sigma} d_{i,m,\sigma} d^\dagger_{i,m',\sigma'} d_{i,m',\sigma'}, \tag{7}$$

$$H_j = \sum_{i,m>m'\sigma,\sigma'} j d^\dagger_{i,m,\sigma} d_{i,m',\sigma} d^\dagger_{i,m',\sigma'} d_{i,m,\sigma'}, \tag{8}$$

$$H_{j'} = \sum_{i,m\neq m'} j' d^\dagger_{i,m,\uparrow} d_{i,m',\uparrow} d^\dagger_{i,m,\downarrow} d_{i,m',\downarrow}, \tag{9}$$

where H_u and $H_{u'}$ are the intra- and inter- orbital Coulomb interactions and H_j and $H_{j'}$ denote the exchange interactions. The term H_j is the origin of the Hund's rule coupling which strongly favors the spin alignment in the same direction on the same atoms. These interactions are expressed by using Kanamori parameters, u, u', j and j' which satisfy the following relations[12,13], $u = U + \frac{20}{9}j$, $u' = u - 2j$ and $j = j'$. Here, U gives a magnitude of the multiplet-averaged d-d Coulomb interaction. The charge-transfer energy Δ, which describes the energy difference between occupied O $2p$ and unoccupied Ti $3d$ levels, is defined by using U and energies of the bare Ti $3d$ and O $2p$ orbitals ε_d^0 and ε_p as follows,

$$\Delta = \varepsilon_d^0 + U - \varepsilon_p, \tag{10}$$

since the characteristic unoccupied $3d$ level energy on the singly occupied Ti site is $\varepsilon_d^0 + U$. The values of Δ, U and $V_{pd\sigma}$ are estimated by photoemission spectra[14,15]. We take the values of these parameters as $\Delta = 6.0$eV, $U = 4.0$eV, $V_{pd\sigma} = -2.0$eV and $j = 0.74$eV throughout the present calculation. The ratio $V_{pd\sigma}/V_{pd\pi}$ is fixed at -2.17 and $V_{pp\sigma}$ and $V_{pp\pi}$ at 0.60eV and -0.15 eV, respectively[16].

Starting with the multi-band Hubbard Hamiltonian, we can derive an effective Hamiltonian in the low-energy region on the subspace of states with singly occupied t_{2g} orbitals at each transition-metal site by utilizing a second-order perturbation theory. The states of $3d$

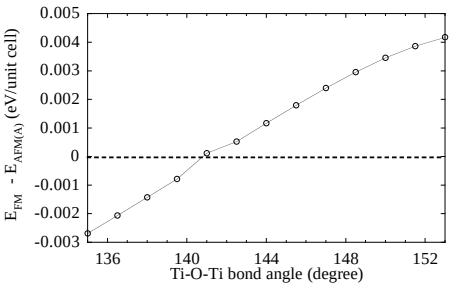

Fig. 2. Relative energy as a function of the Ti-O-Ti bond angle.

electron localized at the transition-metal sites can be represented by two quantum numbers, the z-component of the spin S_z and the number of the occupied orbitals. When one of the two-fold lower t_{2g} orbitals is occupied at each site, we can describe the electronic states using a spin-1/2 operators, which we call the pseudo-spin $\boldsymbol{\tau}$. We follow an approach similar to the well-known Kugel-Khomskii formulation[17, 18, 19, 20]. We express the $3d$ electron operators in terms of $\boldsymbol{S}$ and $\boldsymbol{\tau}$ to arrive at the effective spin and pseudo-spin Hamiltonian;

$$H_{\rm eff} = \tilde{H}_d^{\rm mH} + H_{t_{2g}} + H_{e_g}. \tag{11}$$

The first term $\tilde{H}_d^{\rm mH}$ is obtained from the zeroth-order perturbational processes. The second term $H_{t_{2g}}$ is obtained from the second-order perturbational processes whose intermediate states contain only t_{2g}-orbital degrees of freedom. The third term H_{e_g} is obtained from the second-order perturbational processes whose intermediate states contain e_g-orbital degrees of freedom.

§3. Results

We have calculated the total energies of various spin and orbital configurations by applying a mean-field approximation to the effective spin and pseudo-spin Hamiltonian. Near the AFM-FM phase boundary, the AFM(A) and FM solutions with a certain kind of orbital orderings are stabilized. Figure 2 shows that the AFM(A) to FM phase transition arises by decreasing the Ti-O-Ti bond angle (increasing the $GdFeO_3$-type distortion). In the AFM(A) and FM phases, yz, zx, yz and zx orbitals are predominantly occupied among the two-fold degenerate lower t_{2g} orbitals at site 1, 2, 3 and 4, respectively ((yz, zx, yz, zx)-type orbital order). We can specify the orbital states realized in the AFM(A) and FM solutions by using the angle $\theta_{\rm AFM(A)}$ and $\theta_{\rm FM}$ as,

$$\begin{aligned} &\text{site1;} \quad \cos\theta_x|xy> + \sin\theta_x|yz>, \\ &\text{site2;} \quad \cos\theta_x|xy> + \sin\theta_x|zx>, \end{aligned}$$

$$\begin{aligned} \text{site3}; \quad & -\cos\theta_x|xy> + \sin\theta_x|yz>, \\ \text{site4}; \quad & -\cos\theta_x|xy> + \sin\theta_x|zx>, \end{aligned} \tag{12}$$

where x = AFM(A), FM. In Fig. 3, the angles for the AFM(A) and FM solutions are plotted. The difference between the $\theta_{\rm AFM(A)}$ and $\theta_{\rm FM}$ is very small, especially in the more distorted

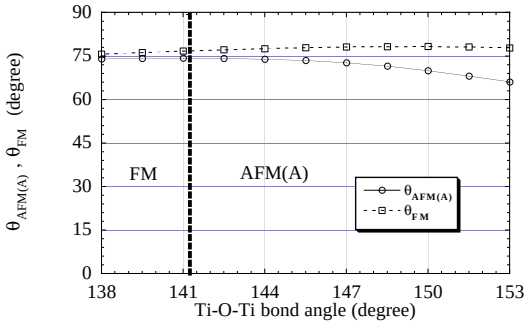

Fig. 3. Orbital states of the FM- and AFM(A) solutions.

region or near the phase boundary. This means that the way of the orbital ordering hardly changes through the magnetic phase transition. Then the AFM(A) to FM phase transition is identified as the transition where the sign of the spin exchange interaction along the c-axis is changed from negative to positive while that in the ab-plane is constantly negative. The constant FM coupling in the ab-plane under the (yz, zx, yz, zx)-type orbital state can be easily understood. In the ab-plane, the neighboring orbitals (yz and zx) are approximately orthogonal to each other. Hence, the FM spin configuration is favored through Hund's coupling interaction. However, the emergence of the FM phase is still controversial since the neighboring orbitals along the c-axis are not orthogonal but have the same symmetries. By considering the transfers from yz to neighboring $3z^2 - r^2$, this is understood schematically as follows.

At this stage, we assume that the (yz, zx, yz, zx)-type orbital order is hardly changed between two phases. Let us consider the energy gain of an electron in the yz orbital at site 1, which is caused by the second-order perturbational processes with respect to the transfers along the c-axis (i.e., the transfers between site 1 and site 3). In the large $GdFeO_3$-type distortion, the yz orbital at site 1 mainly hybridize with the yz and $3z^2 - r^2$ orbitals at site 3 along the z direction relative to the other orbitals. When the yz orbital at site 3 is occupied by an electron, the second-order perturbational energy gain of an electron in the yz orbital at site 1 depends on the spin configuration between site 1 and site 3. When the spins of

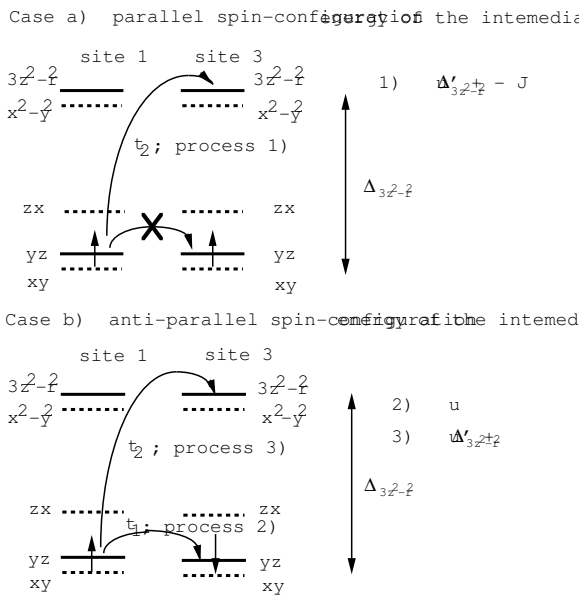

Fig. 4. Characteristic second order perturbational processes.

electrons on site 1 and site 3 are antiparallel, the absolute value of the energy gain can be written approximately as follows(see Fig. 4 a)),

$$\frac{t_1^2}{u} + \frac{t_2^2}{u' + \Delta_{3z^2-r^2}}. \tag{13}$$

Here, t_1 represents the transfer between yz at site 1 and yz at site 3 and t_2 represents that between yz at site 1 and $3z^2 - r^2$ at site 3 and $\Delta_{3z^2-r^2}$ denotes the level-energy difference between $3z^2 - r^2$ and yz orbitals. On the other hand, when the spins are parallel, transfer to the yz orbital is forbidden by Pauli's principle but the energies of the intermediate states in which two electrons occupy the different orbitals are reduced by the intra-site exchange interaction j(see Fig. 4 b)). Consequently, the absolute value of the energy gain can be written as

$$\frac{t_2^2}{u' + \Delta_{3z^2-r^2} - j} \sim \frac{t_2^2}{u' + \Delta_{3z^2-r^2}} + \frac{t_2^2 j}{(u' + \Delta_{3z^2-r^2})^2}. \tag{14}$$

Therefore, the spin configuration between site 1 and site 3 is determined by the competition of following two energies, $\frac{t_1^2}{u}$ and $\frac{t_2^2 j}{(u'+\Delta_{3z^2-r^2})^2}$. In Fig. 5, the values of these energies are plotted as functions of the bond angle. As the $GdFeO_3$-type distortion increases, the indirect hybridizations between neighboring t_{2g} orbitals are decreased and those between neighboring

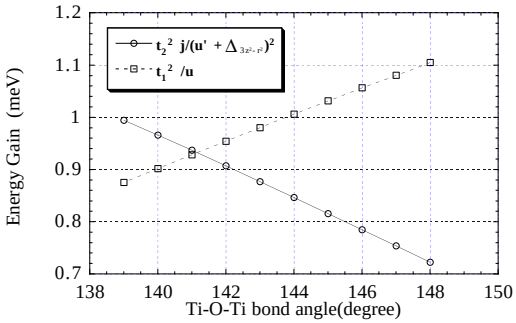

Fig. 5. Characteristic energy gains due to the second order perturbation.

t_{2g} orbitals and e_g orbitals are increased. Consequently, the value of t_1^2/u is decreased and that of $t_2^2 j/(u'+\Delta_{3z^2-r^2})^2$ is increased, resulting in crossing of two energies as the bond angle is decreased. Moreover, since the hybridization between t_{2g} and O $2p$ orbitals becomes to have a σ-bonding character, the amplitudes of the t_2 and $t_2^2 j/(u'+\Delta_{3z^2-r^2})^2$ are critically increased by the $GdFeO_3$-type distortion. Based on the above discussions, we can well describe this system by the following Heisenberg model as far as the (yz, zx, yz, zx)-type orbital order is strongly stabilized and hardly affected by the change of the spin configuration,

$$H_{\rm Heis} = J^c_{\rm Heis} \sum_{\langle i,j \rangle}^{c} \boldsymbol{S}_i \cdot \boldsymbol{S}_j + J^{a,b}_{\rm Heis} \sum_{\langle i,j \rangle}^{a,b} \boldsymbol{S}_i \cdot \boldsymbol{S}_j, \tag{15}$$

with

$$J^{a,b}_{\rm Heis} < 0, \tag{16}$$

$$J^c_{\rm Heis} = 4\left(\frac{t_1^2}{u} - \frac{t_2^2 j}{(u'+\Delta_{3z^2-r^2})^2}\right). \tag{17}$$

Here, $\sum^c_{\langle i,j \rangle}$ denotes the summation over the neighboring spin couplings along the c-axis and $\sum^{a,b}_{\langle i,j \rangle}$ in the ab-plane. The AFM(A) to FM phase transition occurs by the change in the sign of $J^c_{\rm Heis}$. Moreover, within this model, since the value of $J^c_{\rm Heis}$ decreases from a positive value to a negative one continuously as the bond angle is decreased and takes zero at the phase boundary. The two-dimensional spin coupling is realized at the phase boundary. Consequently, the critical temperature at the phase boundary suppressed to zero according to Mermin and Wagner's theorem[21]. Therefore, we can conclude that a strong two-dimensionality in spin couplings is realized near the phase boundary.

In summary, the possible scenario of the rapid decrease of $T_{\rm N}$ is as follows. The $GdFeO_3$-type distortion increases the indirect hybridizations between neighboring t_{2g} and e_g orbitals. As a result, the occupancy of the orbitals directed along c-axis is strongly favored by energy

gain due to the second-order perturbational processes with respect to the transfers in the z-direction. Hence, the (yz, zx, yz, zx)-type orbital order is strongly stabilized almost independently of the spin configuration. Since the orbital structure is hardly changed through the magnetic phase transition, the spin-exchange interaction along the c-axis is decreased from positive value to negative one nearly continuously with decreasing the bond angle, and consequently becomes almost zero at the phase boundary while that in the ab-plane remains constantly ferromagnetic. This strong two-dimensionality at the phase boundary suppresses $T_{\rm N}$ and $T_{\rm C}$ critically. However, a slight change of the orbital state exist at the phase boundary, and it causes the first-order phase transition in this system.

[1] For a review see M. Imada, A. Fujimori and Y. Tokura: Rev. Mod. Phys. **70** (1998) 1039.

[2] J. Akimitsu et. al. unpublished.

[3] J. P. Goral, J. E. Greedan and D. A. Maclean: J. Solid State Chem. **43** (1982) 244.

[4] J. E. Greedan, J. Less-Common Met. **111** (1985) 335.

[5] Y. Okimoto, T. Katsufuji, Y. Okada, T. Arima and Y. Tokura: Phys. Rev. B **51** (1995) 9581.

[6] T. Katsufuji, Y. Taguchi and Y. Tokura: Phys. Rev. B **56** (1997) 10145.

[7] J. P. Goral and J. E. Greedan: J. Magn. Mater. **37** (1983) 315.

[8] J. D. Garret and J. E. Greedan: Inorg. Chem. **20** (1981) 1025.

[9] T. Mizokawa and A. Fujimori: Phys. Rev. B **51** (1995) 12 880.

[10] T. Mizokawa and A. Fujimori: Phys. Rev. B **54** (1996) 5368.

[11] J. C. Slater and G. F. Koster: Phys. Rev. **94** (1954) 1498.

[12] B. H. Brandow: Adv. Phys. **26** (1977) 651.

[13] J. Kanamori: Prog. Theor. Phys. **30** (1963) 275.

[14] T. Saitoh, A. E. Bocquet, T. Mizokawa and A. Fujimori: Phys. Rev. B **52** (1995) 7934.

[15] A. E. Bocquet, T. Mizokawa, K. Morikawa, A. Fujimori, S. R. Barman, K. Mati, D. D. Sarma, Y. Tokura and M. Onoda: Phys. Rev. B **53** (1996) 1161.

[16] W. A. Harrison: Electronic Structure and the Properties of solids (Dover, New York, 1989)

[17] K. I. Kugel and D. I. Khomskii: Pisma. Zh. Eksp. Teor. Fiz. **15**, (1972) 629.

[18] K. I. Kugel and D. I. Khomskii: Zh. Eksp. Teor. Fiz. **64**, (1973) 1429. [Sov. Phys. JETP. **37**, (1973) 725.].

[19] K. I. Kugel and D. I. Khomskii: Sov. Phys. Usp **25**, (1982) 231.

[20] D. I. Khomskii and K. I. Kugel: Solid State Commun. **13**, (1973) 763.

[21] M. D. Mermin and H. Wagner: Phys. Rev. Lett. **17** (1966) 1133.